

## Electronic Supplementary Information

# Rational design of self-assembled surfactant film in nanopipettes: combined fluorescence and electrochemical sensing

Qi Liu, Shushu Ding, Guoyue Shi,\* Anwei Zhu,\*

School of Chemistry and Molecular Engineering, Engineering Research Center of Nanophotonics and Advanced Instrument, Ministry of Education, Shanghai Key Laboratory for Urban Ecological Processes and Eco-Restoration, East China Normal University, 500 Dong Chuan Road, Shanghai 200241, People's Republic of China

\*To whom correspondence should be addressed.

E-mail: [awzhu@chem.ecnu.edu.cn](mailto:awzhu@chem.ecnu.edu.cn); [gyshi@chem.ecnu.edu.cn](mailto:gyshi@chem.ecnu.edu.cn)

Tel: +86-21-54340042; Fax: +86-21-54340042

## Content

1. Experimental Section
2.  $^1\text{H}$  NMR and HR-MS spectra of DIIAQ (Figure S1 and Figure S2)
3. SEM images of the unmodified glass nanopipette tip (Figure S3)
4.  $I$ - $V$  curve of the unmodified glass nanopipette (Figure S4)
5. Contact angle measurement (Figure S5)
6. XPS spectra of S 2p and N 1s (Figure S6)
7. The effect of the incubation time of DIIAQ and SDS (Figure S7)
8. The duration of DIIAQ-SDS in the silanized nanopipette (Figure S8)
9. The self-assembled surfactant film response to Arg (Figure S9)
10. Dual-signal-output for metal optimization (Figure S10)
11. The DIIAQ-SDS system upon titration of Arg (Figure S11)
12. Comparison of different sensors for Arg determination (Table S1)
13. The effect of the SDS/DIIAQ ratio on Arg sensing (Figure S12)
14. Selectivity (Figure S13)

## 1. Experimental Section

### Material and Chemical

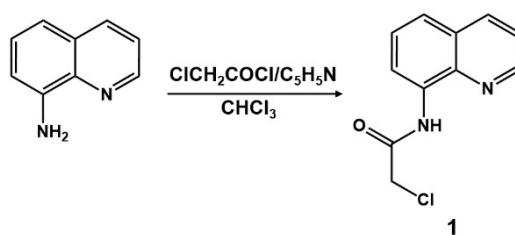
Diethylenetriamine (DETA), bromoacetyl bromide, trifluoroacetic acid, 8-aminoquinoline, 2-chloroacetyl chloride, phenyl tert-butyl carbonate, sodium dodecyl sulfate (SDS), dodecyl trichlorosilane, caesium carbonate, HEPES, 1-methyl imidazole, and all metallic salts were purchased from Aladdin. All of the amino acids including arginine were supported by Sigma Corporation (Germany). Other reagents in the experiment were all of analytical grade. Deionized water (18 M $\Omega$  cm, Hitech science tool laboratory water purification system) was used to obtain the aqueous solutions. All solutions were prepared using ultrapure water from a Milli-Q ultrapure water system.

### Apparatus

Hydrogen nuclear magnetic resonance ( $^1\text{H}$  NMR) spectra was obtained in  $d_6$ -DMSO using the Bruker AV-500 instrument. The highly resolution mass spectra (MS) were acquired using an Agilent 6890 (Agilent, USA). X-ray photoelectric spectroscopy (XPS) was acquired by a Kratos Axis Ultra DLD spectrometer with Al K $\alpha$  source (1486.6 eV). Contact angle was measured using the JC2000A contact angle meter (Zhongchen Digital Technology Co. Ltd., Shanghai, China). The confocal fluorescence images were acquired using a Leica TCS-SP8 confocal laser scanning microscope ( $\lambda_{\text{ex}}$  = 405 nm).

### Synthetic procedures of target DIIAQ

The synthesis process of the imidazolium-derived quinoline-based fluorophore molecule, named DIIAQ, was shown in the [Scheme S1](#) and [Scheme S2](#). The detailed synthesis procedures of the intermediate products were as follows.



**Scheme S1.** Synthesis route of quinoline-derivative **1**.



The reaction process was monitored by thin layer chromatography (TLC). Then, the mixed solution was dissolved with 100 mL of ethyl acetate and the mixture was washed with brine several times. The organic phase was collected and dried over by anhydrous Na<sub>2</sub>SO<sub>4</sub> overnight. Finally, the residue was purified by column chromatography (ethyl acetate/hexane, v/v, 3:1) to afford compound **3** as a yellow solid. <sup>1</sup>H NMR (δ ppm, 500 MHz, CDCl<sub>3</sub>): 10.34 (s, 1H), 8.83 (m, 2H), 8.24 (d, J = 8.0 Hz, 1H), 7.59 (d, 2H), 7.50 (m, 1H), 4.86 (s, 2H), 3.69 (m, 2H), 3.53 (m, 4H), 3.37 (m, 2H), 1.41 (s, 18H). ESI-MS (m/z) (C<sub>25</sub>H<sub>37</sub>N<sub>5</sub>O<sub>5</sub>): calculated [(M + H)], 488.29; found, 488.2867.

Synthesis of Compound **4**. Trifluoroacetic acid (9.4 mL, 100 mmol) was added dropwise to the CH<sub>2</sub>Cl<sub>2</sub> solution (18 mL) containing 0.68 g Compound **3** (1.4 mmol) and the reaction solution was stirred at room temperature overnight. Then, the mixed solution was concentrated and dissolved in 10 mL of water. The aqueous was modulated to pH ~9 with saturated sodium carbonate solution and extracted with chloroform. The organic layer was collected and dried with anhydrous Na<sub>2</sub>SO<sub>4</sub> overnight. The residue was evaporated to obtain the final product, which was directly used for the next reaction.

Synthesis of Compound **5**. Compound **4** (0.14g, 0.49mmol) was dissolved in 35 mL dichloromethane containing 0.28 mL triethylamine at 0°C. The solution of bromoacetyl bromide (0.17 mL, 20 mmol) in 15 mL CH<sub>2</sub>Cl<sub>2</sub> was added dropwise for about 30 min at ice bath, and then the mixture was stirred at room temperature for 2 days. The reaction process was monitored by TLC. Next, the mixed solution was washed with water for three times and dried over by anhydrous Na<sub>2</sub>SO<sub>4</sub>. After the concentration, the residue was purified by column chromatography (dichloromethane/methyl alcohol, v/v, 20:1) to obtain a yellow solid. <sup>1</sup>H NMR (δ ppm, 500 MHz, CDCl<sub>3</sub>): 10.38 (NHCO, s, 1H), 8.85 (d, J = 8.0 Hz, 1H), 8.80 (d, J = 8.6 Hz, 1H), 8.32 (d, J = 8.0 Hz, 1H), 7.65 (m, 2H), 7.57 (d, J = 8.0 Hz, 1H), 4.96 (2H), 3.87 (s, 4H), 3.73 (s, 4H), 3.58 (s, 4H). ESI-MS (m/z) (C<sub>19</sub>H<sub>23</sub>Br<sub>2</sub>N<sub>5</sub>O<sub>3</sub>): calculated [(M + Na)<sup>+</sup>], 550.01; found, 550.0060.

Synthesis of the target Compound **DIIAQ**. 1-methyl imidazole and compound **5** (0.04g, 0.076mmol) were dissolved in 10 mL dry tetrahydrofuran. The resulting solution was refluxed for 3 days under nitrogen and monitored by TLC. Then, the reaction solution was filtered, and the solid was heated in acetone for 8 h under reflux. At last, the solid produce was filtered and washed with ether to afford the final compound **DIIAQ**. <sup>1</sup>H NMR (δ ppm, 400 MHz, CDCl<sub>3</sub>): 10.48 (NHCO, s, 1H), 9.05 (s, 1H), 8.93 (d, J = 8.0 Hz, 2H), 8.60 (d, 1H), 8.45 (d, J = 8.0 Hz, 1H), 7.74 (m, 5H), 7.60 (m, 4H), 5.01 (s, 2H), 4.95 (s, 2H), 4.90 (s, 2H), 3.87 (s, 6H), 3.51 (t, J = 8.0 Hz, 4H), 3.36 (t, J = 8.0 Hz, 4H). ESI-MS (m/z) (C<sub>27</sub>H<sub>35</sub>N<sub>9</sub>O<sub>3</sub><sup>2+</sup>) calculated [(M - H)], 532.28; found, 532.2779.

### Preparation of Nanopipette System

The conical glass nanopipettes were provided using the borosilicate capillary glasses (i.d. = 0.78 mm; o.d. = 1 mm) which was obtained from Sutter P-2000 micropipette

puller Instrument. The specific preparation process was as follows: first, the borosilicate capillary glasses were ultrasonic cleaned for 2 h using the freshly prepared piranha solution (the ratio of 98% H<sub>2</sub>SO<sub>4</sub>/30% H<sub>2</sub>O<sub>2</sub> was 3:1) to wipe off the impurities on the capillary glasses. After that, the capillaries were rinsed with plenty of distilled water and vacuum dried at 80 °C. Then, the glasses were pulled by a Sutter P-2000 micropipette puller with the following parameters: heat = 275; Fil = 4; Vel = 20; Del = 140; Pull = 150.

Next, the glass nanopipettes were modified through a series of chemical processes. Firstly, 10 mL of anhydrous toluene and 0.25 mL of dodecyl trichlorosilane were mixed to a 25 mL reaction flask with a stopper. The solution was ventilated with argon for 30 min. Then, the above-mentioned mixed solution was injected into the nanopipette with a micro-injector and the nanopipettes were putted into the reaction flask quickly. The reaction flask was vacuumized and filled with argon repeatedly for three times and the nanopipettes were leaved at room temperature for 12 h. After that, the above nanopipettes were washed with methanol to remove dodecyl trichlorosilane physically adsorbed on the inner wall of nanopipette, and vacuum dried for 4 h at 60°C. Finally, compound DIIAQ and SDS were modified through self-assembly with alkane chains on the inner wall of the nanopipettes at 30 °C for 16 h.

### **Ion Current Measurement**

The *I-V* curves were measured by an electrochemical instrument (CHI 660C, Chenhua Co., Shanghai, China). In order to detect ion current through the glass nanopipettes, we used one Ag|AgCl electrode acting as the external reference/auxiliary electrode and another Ag|AgCl electrode was used to insert in the internal of the glass nanopipette as a working electrode. All aqueous solutions were prepared from Milli-Q water (18.2 MΩ cm at 25 °C). The buffer solution was 10 mM HEPES (pH = 7.4) solution containing 10 mM KCl as the supporting electrolyte throughout the work. The scanning voltage range was from -1.0 V to +1.0 V. Repeated three times for each experiment.

### **Age-related Difference in Plasma Arginine Metabolism**

All procedures involving animals were approved by the Animal Ethics Committee of East China Normal University, China (No. m20190702). APP/PS1 transgenic mice at 7 and 13 months of age were purchased from the Shanghai Research Center for Model Organisms. The mice were housed in a light-controlled (12 h on/12 h off) and temperature-controlled environment and provided ad libitum access to food and water. For each animal, after being anesthetized with sodium pentobarbital, retro-orbital sinus blood samples were collected in an EDTA-coated tube and stored on ice. The EDTA tubes were centrifuged at 2000 rpm for 10 min at 4 °C (Eppendorf 5418) and the plasma was then collected. The plasma samples were diluted 10<sup>6</sup> times with buffer solution (10 mM HEPES, pH 7.4) for the subsequent measurements.

## 2. <sup>1</sup>H NMR and HR-MS spectra of DIIAQ

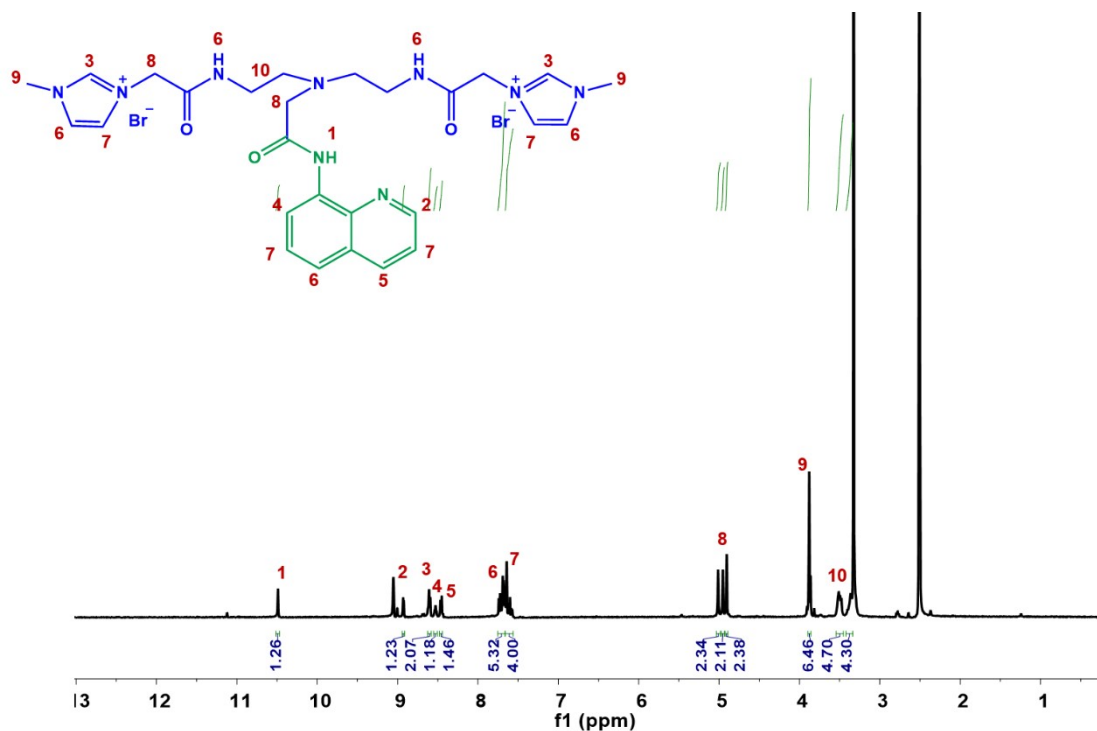


Figure S1. <sup>1</sup>H NMR spectrum of DIIAQ obtained in d<sub>6</sub>-DMSO.

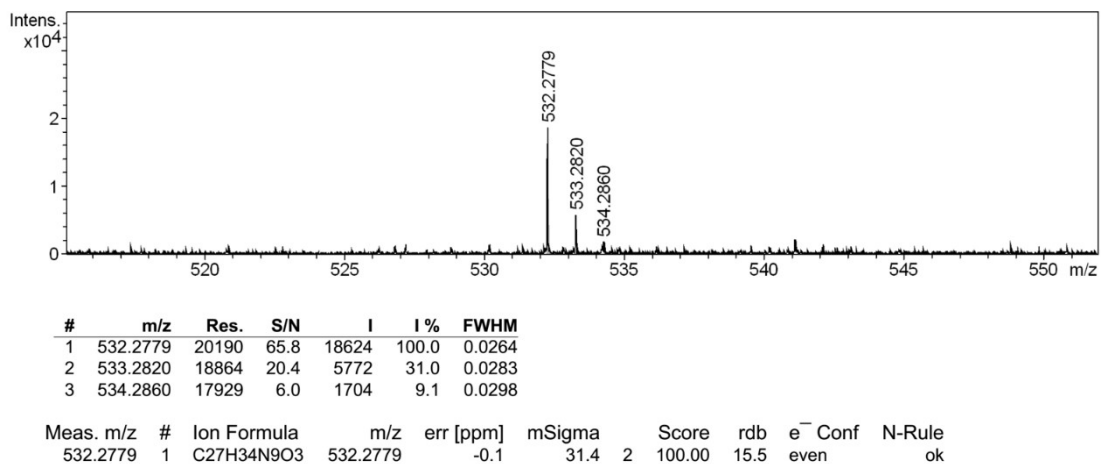
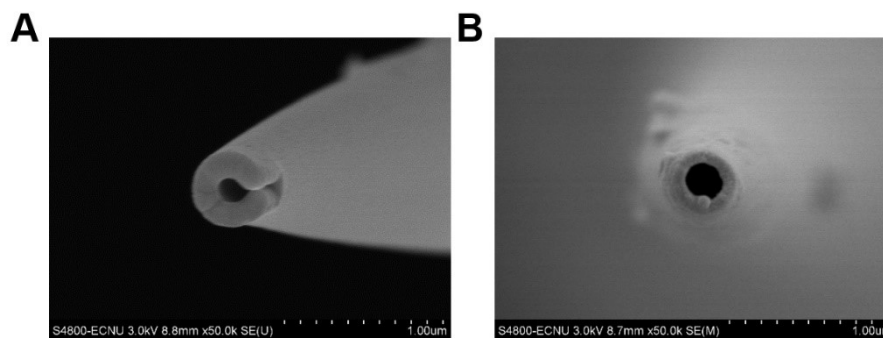


Figure S2. HR-MS spectrum of DIIAQ.

### 3. SEM images of the unmodified glass nanopipette tip



**Figure S3.** SEM images of the unmodified glass nanopipette tip from different angles.



#### 4. *I-V* curve of the unmodified glass nanopipette

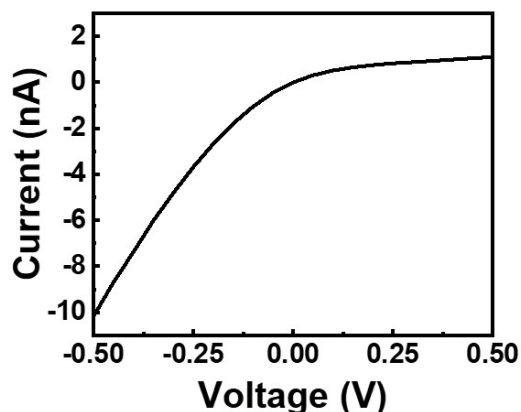


**Figure S4.** *I-V* curve of bare glass nanopipette in 0.1 M KCl solution that HEPES (10 mM) was the buffer solution (pH = 7.4). The nanopipette size calculated by electrochemical measurement was ~180 nm.

The orifice size of the glass nanopipette could be estimated from electrochemical measurements based on eqn (1)<sup>3</sup>.

$$r = \frac{1}{\pi \kappa R \tan \frac{\theta}{2}} \quad (1)$$

where  $r$  is the orifice radius of the glass nanopipette;  $\kappa$  is the conductivity of the electrolyte solution (1.2 S/m for 0.1 M KCl);  $R$  is the measured resistance of the nanopipette and  $\theta$  is the cone angle. The inner size of nanopipette was estimated to be ~180 nm from the electrochemical measurement, which was consistent with the scanning electron microscope (SEM) image.

## 5. Contact angle measurement

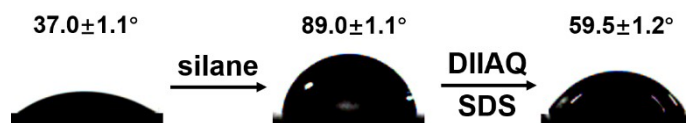


**Figure S5.** Contact angle measurement of the droplet profile on the flat glass simulating the modification process of the Arg sensing system.

As shown in Fig. S5, the contact angle decreased from  $\sim 89.0^\circ$  to  $\sim 59.5^\circ$  after being treated by SDS and DIIAQ, showing a more hydrophilic surface, explaining the changes in interface wettability.

## 6. XPS spectra of S 2p and N 1s

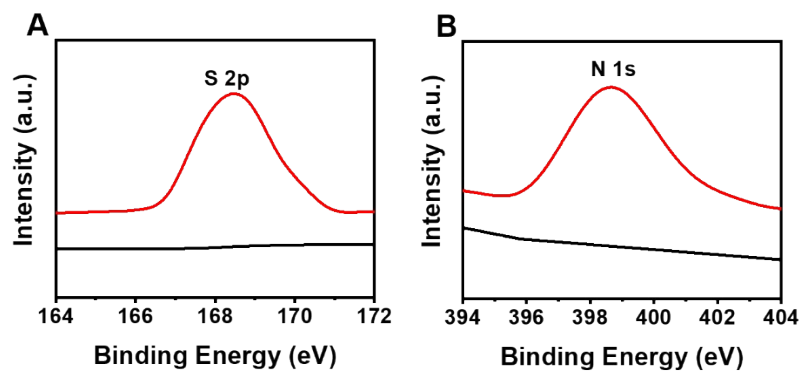


**Figure S6.** Flat glass was used to simulate the modification process of the DIIAQ in the inner wall of the nanopore. XPS spectra of **A** (S 2p) and **B** (N 1s) characteristic peak at 168.5 eV and 398.6 eV respectively of the fluorescence probe.

## 7. The effect of the incubation time of DIIAQ and SDS

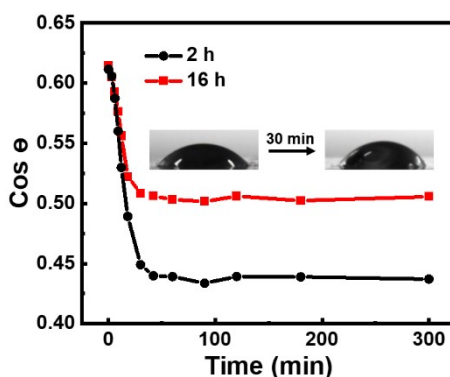


**Figure S7.** Contact angles of pure water on DIIAQ-SDS modified flat glass slide after soaking in buffer solution with different time. The silane-glass slides were pre-incubated with SDS and DIIAQ with 2 h (black line) or 16 h (red line). Inset: water drop profiles on the surfactant film modified planar glass slide surface (16 h preincubation times with SDS and DIIAQ) before and after 30 min equilibration in buffer solution.

As shown in Fig. S7, after 16 h incubation time in 8 mM SDS and 40  $\mu$ M DIIAQ, the initial contact angle of pure water on DIIAQ-SDS modified flat glass was 52° (red line and inset image). Although the subsequent immersion of the modified flat glass in buffer solution (10 mM HEPES solution containing 10 mM KCl, pH = 7.4) changed the contact angle with time, it can reach equilibrium with a contact angle of 59.5° at about 30 min (red line and the inset). The change of contact angle was due to the desorption of DIIAQ and/or SDS into solution. If the initial incubation time of SDS and DIIAQ was reduced to 2 h (Fig. S7, black line), the initial contact angle of pure water on surfactant film modified flat glass was almost the same, but it became more hydrophobic after the immersion the glass in buffer solution (10 mM HEPES solution containing 10 mM KCl, pH = 7.4) for the same time, implying more SDS and DIIAQ desorbed. Therefore, the longevity of the sensor film was affected by the modification time of SDS and DIIAQ and the sensor should be incubated with the buffer solution for equilibration before use. In this work, we chose 16 h for the initial incubation time in

SDS and DIIAQ and all measurements were carried out after 30 min equilibration time in buffer.

## 8. The duration of DIIAQ-SDS in the silanized nanopipette

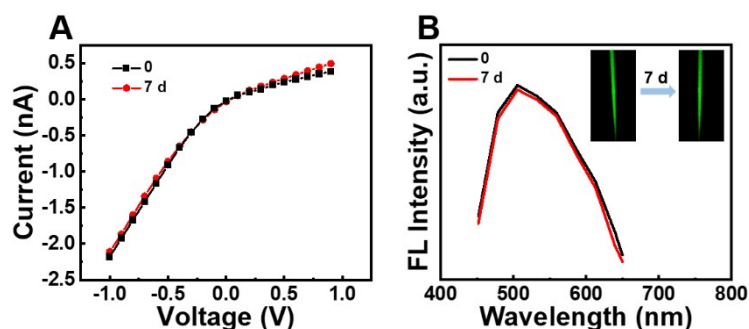


**Figure S8.** **A**  $I$ - $V$  curves of the freshly prepared DIIAQ-SDS modified nanopipette before and after being placed in buffer solution at room temperature for 7 days; **B** Fluorescence emission spectra of the decorated nanopipette at 0 and 7 days of age. Inset: fluorescence images of the DIIAQ-SDS decorated nanopipette at 0 and 7 days of age. 10 mM HEPES solution containing 10 mM KCl as the buffer solution (pH 7.4). Fluorescence measurement was carried by confocal laser scanning microscopy under 405 nm excitation and 450-650 nm collection.

In order to investigate the longevity of sensor film in nanopipettes, the nanopipettes were stored in buffer solution at room temperature for 7 days. We evaluated the electrochemical performance of the 7 day-aged DIIAQ-SDS modified nanopipette. The  $I$ - $V$  curves of fresh prepared nanopipette and 7 days aged nanopipette were recorded respectively. Compared with the freshly prepared nanopipette, the nanopipette showed an almost unchanged ion current at -1 V after placing for 7 days (Fig. S8A). Besides, due to the introduction of fluorescent DIIAQ, fluorescent measurement by the confocal laser scanning microscopy can also be used to study the lifetime of DIIAQ-SDS on the internal wall of silane-nanopipette. It is evident that no remarkable change was noticed in the fluorescence intensity (Fig. S8B) and fluorescence images (Fig. S8B, inset) of nanopipette, which confirmed that the surfactant film modified in the nanopipette were not destroyed.

## 9. The self-assembled surfactant film response to Arg

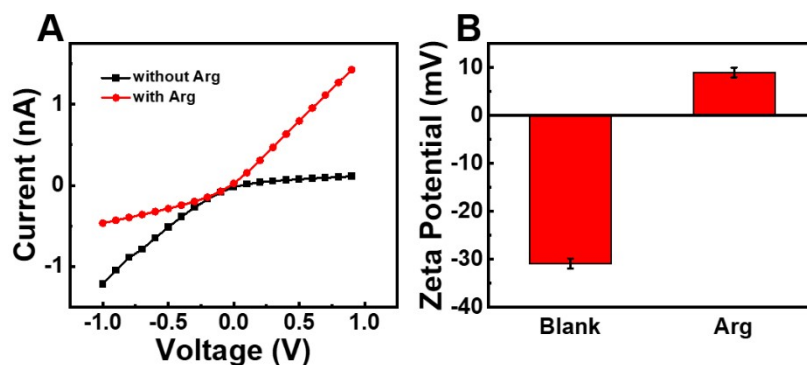


**Figure S9.** **A** *I*-*V* curves of the DIIAQ-SDS-Cu<sup>2+</sup> decorated nanopipette response to 1 pM Arg; **B** Surface zeta ( $\zeta$ ) potential of the DIIAQ-SDS-Cu<sup>2+</sup> modified flat glass before and after treated with Arg. The buffer solution: 10 mM HEPES containing 10 mM KCl, pH 7.4.

As shown in Fig. S9B, the surface became positive instead of being more negative after adding Arg to the DIIAQ-SDS-Cu<sup>2+</sup> modified interface, proving the binding of Arg with DIIAQ-SDS-Cu<sup>2+</sup>.

## 10. Dual-signal-output for metal optimization

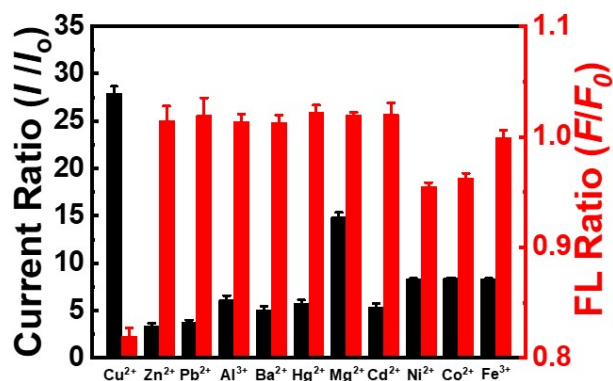


**Figure S10.** The ion current ratio ( $I/I_0$ ,  $I_0$  and  $I$  were the ion currents at +1 V before and after treated by Arg) and fluorescence intensity ratio ( $F/F_0$ ,  $F_0$  and  $F$  were the average fluorescence intensities before and after treated by Arg) of DIIAQ-SDS- $M^{n+}$  (40  $\mu$ M/8 mM/35  $\mu$ M) modified nanopipette upon the treatment of Arg (Fluorescence measure was carried by confocal laser scanning microscopy under 405 nm excitation and 450–650 nm collection,  $M^{n+}$  refers to various metal ions listed in the figure). The buffer solution was 10 mM HEPES (pH = 7.4) solution containing 10 mM KCl as the supporting electrolyte.



## 11. The DIIAQ-SDS system upon titration of Arg

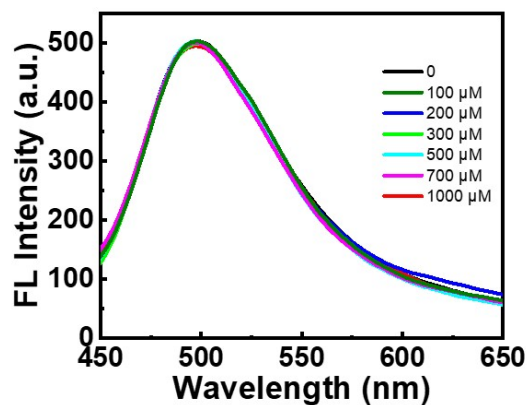


**Figure S11.** Fluorescence emission spectra of DIIAQ-SDS system upon titration of Arg in the absence of  $\text{Cu}^{2+}$  by liquid-phase fluorometric assay ( $[\text{DIIAQ}] = 40 \mu\text{M}$ ;  $[\text{SDS}] = 8 \text{ mM}$ ). The fluorescence emission spectra were obtained from the TECAN microplate reader, using a black 384 well microplate.  $\lambda_{\text{ex}} = 405 \text{ nm}$ .

## 12. Comparison of different sensors for Arg determination

**Table S1** Comparison of the detection limit of different sensors for the determination of Arg

Method	Linear range ( $\mu\text{M}$ )	Limit of detection ( $\mu\text{M}$ )	Ref.
Colorimetric and fluorometric dual-signal sensor	0.1 - 5	$3.7 \times 10^{-2}$	4
Graphene-based FET	10 - 1000	< 10	5
Organic Framework Luminescent Sensor	0 - 220	1.06	6
Ratiometric fluorescence sensor	0 - 160	$1.5 \times 10^{-2}$	7
Amperometric biosensor based on polyaniline-modified electrode	70 - 600	38	8
Self-assembled surfactant film in nanopipettes	$10^{-6}$ - $10^{-2}$	$10^{-6}$	This work

### 13. The effect of the SDS/DIIAQ ratio on Arg sensing

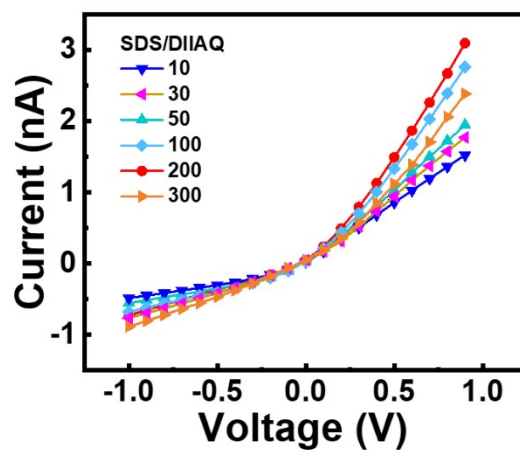


**Figure S12.** *I*-*V* curves of the nanopipette system response to 1 nM Arg in an adjustable molar ratio of SDS/DIIAQ (10, 30, 50, 100, 200, 300) in 10 mM HEPES containing 10 mM KCl (pH 7.4).

## 14. Selectivity

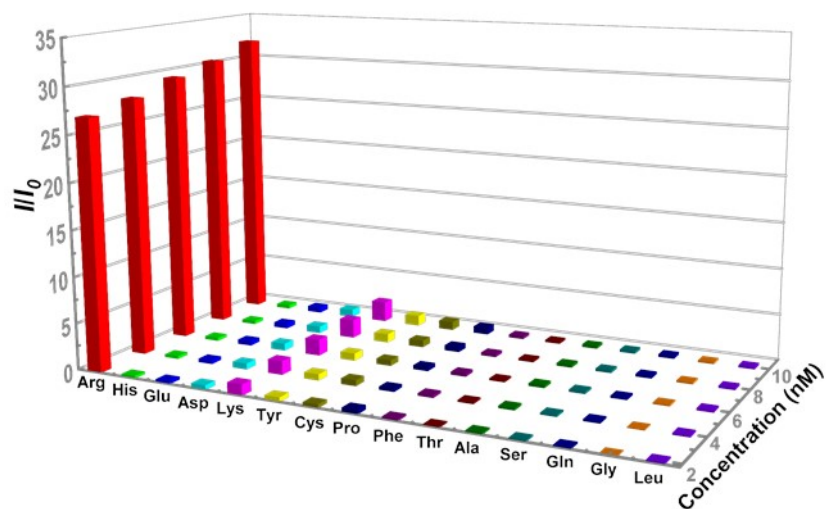


**Figure S13.** Ion current ratio ( $I/I_0$ ) of DIIAQ-SDS- $\text{Cu}^{2+}$  modified nanopipette upon addition of various amino acids including Arg from 2 to 10 nM ([DIIAQ] =  $40 \mu\text{M}$ ; [SDS] = 8 mM; [ $\text{Cu}^{2+}$ ] =  $35 \mu\text{M}$ ; 10 mM HEPES solution containing 10 mM KCl as the buffer solution, pH 7.4).

## Reference

- (1) Y. Zhang, X. Guo, W. Si, L. Jia and X. Qian, *Org. Lett.*, 2008, **10**, 473-476.
- (2) C. P. Holmes, A. Chakrabarti, B. T. Frederick, Y. Pan, Y. S. Dong and A. Bhandari, U.S. Patent 8106154B2, Aug 07, 2008.
- (3) S. Cao, S. Ding, Y. Liu, A. Zhu and G. Shi, *Anal. Chem.*, 2017, **89**, 7886-7892.
- (4) T. Liu, N. Li, J. X. Dong, Y. Zhang, Y. Z. Fan, S. M. Lin, H. Q. Luo and N. B. Li, *Biosens. Bioelectron.*, 2017, **87**, 772-778.
- (5) T. Berninger, C. Bliema, E. Piccinini, O. Azzaroni and W. Knoll, *Biosens. Bioelectron.* 2018, **115**, 104-110.
- (6) L. Wang, B. Tu, W. Xu, Y. Fu and Y. Zheng, *Inorg. Chem.*, 2020, **59**, 5004-5017.
- (7) H. Q. Yin, X. Y. Wang and X. B. Yin, *J. Am. Chem. Soc.*, 2019, **141**, 15166-15173.
- (8) N. Stasyuk, O. Smutok, G. Gayda, B. Vus, Y. Koval'chuk and M. Gonchar, *Biosens. Bioelectron.*, 2012, **37**, 46-52.